Energy Transfer through Heterogeneous Dyes-Substituted Fluorene-Containing Alternating Copolymers and Their Dual-Emission Properties in the Films

Hyeonuk Yeo, Kazuo Tanaka*, Yoshiki Chujo*

Department of Polymer Chemistry, Graduate School of Engineering, Kyoto University, Katsura, Nishikyo-ku, Kyoto 615-8510, Japan

chujo@chujo.synchem.kyoto-u.ac.jp

KEYWORDS

dual emission, energy transfer, fluorene, cardo structure

Graphical abstract:

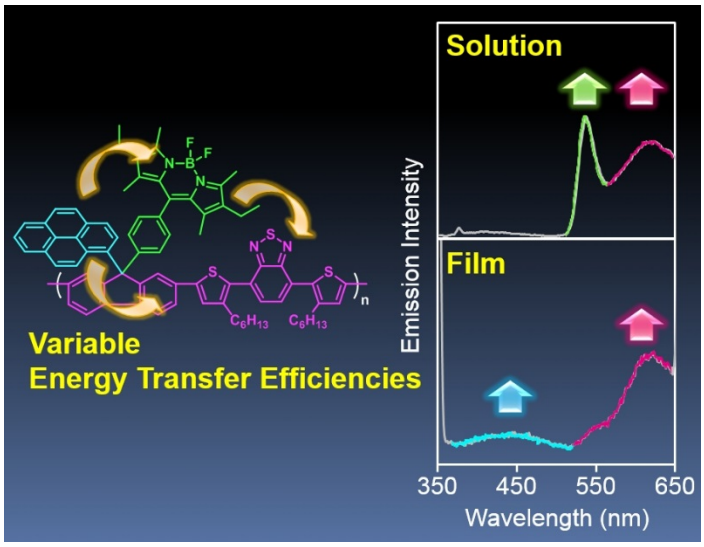

A series of the alternating fluorene copolymers modified with pyrene or 9,10-diphenylanthracene and BODIPY at the cardo carbon based on the red-emissive donor-acceptor structure were prepared. From the measurements of the optical properties, the energy transfer efficiencies were evaluated. In summary, variable energy transfer efficiencies were observed between the side chains and from the side chain to the main chain. Finally, the dual-emissive polymers were obtained in the film states.

ABSTRACT

We report synthesis of the modified fluorene polymers tethered to the heterogeneous types of the fluorescent dyes at the cardo carbon for obtaining the dual-emissive solid materials. A series of the alternating fluorene copolymers modified with pyrene or 9,10-diphenylanthracene and BODIPY at the cardo carbon based on the red-emissive donor-acceptor structure were prepared, and their characteristics were examined. From the measurements of the optical properties, the energy transfer efficiencies were evaluated. In summary, variable energy transfer efficiencies were observed between the side chains and from the side chain to the main chain. It was indicated that the energy transfer efficiencies were strongly depended on the types of the energy donor and the detection conditions such in the solution or film. Furthermore, it was found that the cardo fluorene units can contribute to the suppression of the energy transfer in the condensed state. Finally, the dual-emissive polymers were obtained in the film states. This is the first example, to the best of our knowledge, not only to offer systematic information on the energy transfer between the dye molecules and the polymer main-chains via the cardo structure but also to demonstrate the polymer-based optical materials with the dual-emission properties.

INTRODUCTION

The fluorene-based alternating polymers are commodity materials for fabricating modern organic opto-electronic devices. As an emissive materials, a wide variety of fluorene-based functionalized polymers have been developed for the application to the electroluminescence devices.[1−3] By connecting fluorene with the functional units, color tuning was demonstrated.[4−6] As another instance, by the conjugation with the strong electron-accepting unit such as benzothiadiazole or organometallic complexes, the donor−acceptor interaction can be formed at the excited state.[7−11] Since these electronic states are feasible in encouraging charge separation and suppressing recombination, the fluorene-based polymers having the CT property are used as a key material in the bulk-heterojunction in the photovoltaic cells.[12,13] Thus, the development of the new functional polymers using fluorene are still a current topic with high relevance.

We have also focused on the potential applications of the cardo fluorene structure as a building block for constructing the multi-functional optical materials based on the preprogrammed design.[14−16] It is presumed that the cardo structure in the dye-tethered fluorene could provide the suitable scaffold for obtaining the intrinsic characteristics of the dyes without loss of emission properties. Indeed, we have recently reported that the cardo carbon can play a role in the isolation from the electronic interaction in polyfluorenes.[14] The optical properties of the main-chain conjugation through the cardo polyfluorenes can be preserved from the influence of the electron-withdrawing and donating groups tethered to the polyfluorene via the cardo carbons. Consequently, it was demonstrated that a series of the modified polyfluorenes provided the pure-blue emissions.[15] In addition, the concentration quenching which is the crucial obstacle for preparing highly-bright emissive devices can be suppressed by tethering the fluorophores to polyfluorene via the cardo carbon.[15] With boron dipyrromethene (BODIPY) which readily forms the aggregation and shows the concentration quenching, the bright emissions were obtained after the accumulation onto the polyfluorene main-chains. Strong green emissions originated from the BODIPY units can be observed without significant losses of emission quantum efficiencies.

Moreover, we found the inefficient energy transfer between the dye at the side chains and the polymer main-chains composed of the donor-acceptor alternating sequences.[15] Furthermore, the dual emission which should show the two kinds of emissions from a single material in the different wavelength regions with the excitation at the single wavelength light was realized from a single polymer component in the solution state.[16] These polymers are versatile not only for preparing optical devices[17,18] but also for applying to the bio-sensors.[19–21] However, the mechanism for the insufficient energy transfer between BODIPY and the polymer main-chain is still unclear because there are very few other examples on the energy transfer between the dyes tethered to the cardo carbons. The electronic structures of the cardo fluorenes modified by various kinds of dyes are not assessed in detail yet. In addition, dual-emission behaviors were lost at the condensed state, resulting in the monotonous emission in the film state. To extend the versatility of the cardo fluorene as an optical material, the systematic information on the energy transfer between the side-chains as well as between the side-chain and the main-chain should be strongly required.

Herein, we report the modified fluorene polymers tethered to the heterogeneous types of the fluorescent dyes at the cardo carbon and their dual-emissive properties in the film state. Initially, we synthesized the desired polymers and collect the information on the energy transfer between the dye molecules and the polymer main-chains via the cardo structure, we prepared a series of the modified fluorenes tethered to the heterogeneous types of the fluorescent dyes at the cardo carbon as a monomer with pyrene, 9,10-diphenylanthracene (DPA), and/or BODIPY. The alternative polymers with the red emission were synthesized via the metal-catalyzed polymerization using the dithiophenylbenzothiadiazole (TBT) unit. From the comparison of the optical properties of the synthesized compounds, the energy transfer efficiencies were evaluated in the solution and the film states. Finally, the dual-emissive films were successfully obtained. This is the first example, to the best of our knowledge, not only to offer systematic information on the energy transfer between the dye

molecules and the polymer main-chains via the cardo structure but also to demonstrate the polymer-based optical materials with the dual-emission properties.

Experimental section

General. ^{1}H NMR, ^{13}C NMR and ^{11}B NMR spectra were measured with a JEOL EX-400 (400 MHz for ^{1}H, 100 MHz for ^{13}C, 128 MHz for ^{11}B) spectrometer (JEOL Ltd., Tokyo, Japan). Coupling constants (*J* value) are reported in Hertz. ^{1}H and ^{13}C NMR spectra used tetramethylsilane (TMS) as an internal standard, ^{11}B NMR were referenced externally to $BF_3{\cdot}OEt_2$ (sealed capillary) in $CDCl_3$. The number−average molecular weight (M_n) and the polydispersity index (PDI) [weight-average molecular weight/number-average molecular weight (M_w/M_n)] of all polymers were estimated by size-exclusion chromatography (SEC), performed on a TOSOH G3000HXI system equipped with three consecutive polystyrene gel columns [TOSOH gels: α−4000, α−3000, and α−2500] and an ultraviolet detector at 40 °C. The system was operated at a flow rate of 1.0 mL/min with $CHCl_3$ as an eluent. The system was calibrated with polystyrene standards. UV−Vis spectra were recorded on a Shimadzu UV−3600 spectrophotometer. Fluorescence emission spectra were recorded on a HORIBA JOBIN YVON Fluoromax−4 spectrofluorometer, and the absolute quantum yield was calculated with the integrating sphere on the HORIBA JOBIN YVON Fluoromax−4 spectrofluorometer in chloroform. Fluorescence lifetime analysis was carried out on a HORIBA FluoreCube spectrofluorometer system; excitation at 290 nm was carried out using a UV diode laser (NanoLED-290L).

Materials. Tetrahydrofuran (THF), diethyl ether (Et_2O), and triethylamine (Et_3N) were purified using a two-column solid-state purification system (Glasscontour System, Joerg Meyer, Irvine, CA). Pyrene and 9,10-diphenylanthracene were obtained commercially, and used without further purification. 4-(2,7-Dibromo-9-hydroxy-9H-fluoren-9-yl)benzaldehyde (**1**), 2,7-dibromo-9-[4-(octyloxy)phenyl]-9H-fluoren-9-ol (**4**), 4,7-bis[4-hexyl-5-(trimethylstannyl)thiophen-2-yl]benzo[c][2,1,3]-thiadiazole, 2,6-diethyl-4,4-difluoro-1,3,5,7-tetramethyl-8-phenyl-4-bora-3a,4a-diaza-s-indacene, polymer **PF-BO-TBT** and **PF-TBT** were prepared according to the literature.[14−16] All reactions were performed under argon atmosphere.

4-(2,7-Dibromo-9-(pyren-1-yl)-9H-fluoren-9-yl)benzaldehyde (2). Trifluoromethanesulfonic acid (2.53 g, 16.9 mmol) was slowly added to a dioxane solution (35 mL) of **1** (5.00 g, 11.3 mmol) and pyrene (2.73 g, 13.5 mmol). After stirring at 70 °C for 6 h, the resulting mixture was diluted with saturated aqueous $NaHCO_3$. Then, the product was extracted with cyclopentyl methyl ether (CPME). The combined organic extracts were washed with brine and dried over anhydrous Na_2SO_4. After removing the solvent, the crude product was purified by silica gel column chromatography (8 : 1 = hexane : EtOAc, R_f = 0.20) to afford the product **2** (5.50 g, 77%) as a yellow solid. ^{1}H NMR ($CDCl_3$, ppm) 9.98 (s, 1H), 8.21 (d, *J* = 7.5, 1H), 8.14 (d, *J* = 7.4 Hz, 1H), 8.08 (d, *J* = 8.7 Hz, 1H), 8.05−7.97 (m, 3H), 7.86 (br, 1H), 7.77 (d, *J* = 8.3 Hz, 2H), 7.70 (br, 3H), 7.62 (br, 1H), 7.55 (dd, *J* = 8.2 Hz, 1.5 Hz, 2H), 7.34 (d, *J* = 8.2 Hz, 2H). ^{13}C NMR ($CDCl_3$, ppm) 191.5, 138.0, 137.8, 135.2, 131.6, 131.4, 131.2, 130.6, 130.1, 129.5, 129.1, 129.0, 128.2, 127.9, 127.3, 127.0, 126.5, 126.3, 126.0, 125.7, 125.4, 125.3, 125.1, 124.8, 123.4, 122.2, 121.9, 67.1. HRMS (p-APCI) calcd. for $C_{36}H_{20}Br_2O+H^+$: m/z 628.9944; found: m/z 628.9925.

4-(2,7-Dibromo-9-(4-(10-phenylanthracen-9-yl)phenyl)-9H-fluoren-9-yl)benzaldehyde (3). Similarly to the preparation of **2**, compound **3** was prepared from **1** (4.44 g, 10.0 mmol) and 9,10-diphenylanthracene (3.63 g, 11.0 mmol) in the presence of trifluoromethanesulfonic acid (2.24 g, 15.0 mmol) in 64% yield as a pale yellow solid (4.84 g). ^{1}H NMR ($CDCl_3$, ppm) 9.95 (s, 1H), 7.75−7.71 (m, 2H), 7.70−7.65 (m, 2H), 7.60−7.53 (m, 2H), 7.52−7.49 (m, 2H), 7.47−7.43 (m, 4H), 7.42−7.38 (m, 4H), 7.33−7.29 (m, 2H), 7.28−7.24 (m, 3H), 7.22−7.18 (m, 2H). ^{13}C NMR ($CDCl_3$, ppm) 191.6, 151.5, 150.7, 139.1, 138.6, 138.1, 138.0, 137.5, 136.9, 135.3, 131.2, 130.8, 130.23, 130.15, 130.0, 129.3, 129.1, 128.8, 128.6, 128.4, 128.2, 127.9, 127.6, 127.3, 127.0, 125.5, 125.3, 125.1, 121.9, 121.7, 65.7. HRMS (p-APCI) calcd. for $C_{46}H_{28}Br_2O+H^+$: m/z 757.0559; found: m/z 757.0555.

Monomer F-PY-BO. A flask charged with 70 mL of dichloromethane was degassed with argon for 1 h, and **2** (1.58 g, 2.51 mmol), 2,4-dimethyl-3-ethyl-1H-pyrrole (0.62 g, 5.01 mmol), and two drops of trifluoroacetic acid (TFA) were placed. After stirring for 4 h at room temperature, to the solution was added 2,3-dichloro-5,6-dicyano-*p*-benzoquinone (DDQ) (0.62 g, 2.73 mmol). After stirring for additional 3 h at room temperature, triethylamine (5 mL) and $BF_3{\cdot}OEt_2$ (7 mL) were added. After stirring overnight, the solution was evaporated. After flash chromatography on silica gel (8 : 1 = hexane : ethyl acetate, R_f = 0.4), recrystallization by hexane provided **F-PY-BO** (0.35 g, 15%) as a red powder. ^{1}H NMR ($CDCl_3$, ppm) 8.20 (t, *J* = 5.1, 2H), 8.10-8.00 (m, 5H), 7.83 (d, *J* = 9.1 Hz, 1H), 7.69 (d, *J* = 8.4 Hz, 2H), 7.64 (m, *J* = 8.3 Hz, 1H), 7.54 (dd, *J* = 7.9 Hz, 2.0 Hz, 2H), 7.28 (d, *J* = 8.3 Hz, 2H), 7.17 (d, *J* = 8.7 Hz, 2H), 2.53 (s, 3H), 2.49 (s, 3H), 2.40 (q, *J* = 7.2 Hz, 2H), 2.25 (q, *J* = 7.2 Hz, 2H), 1.68 (br, 3H), 1.06 (m, 6H), 0.93 (t, *J* = 7.5 Hz, 3H). ^{13}C NMR ($CDCl_3$, ppm) 153.8, 153.7, 153.4, 147.1, 139.6, 138.3, 138.0, 136.6, 134.7, 132.9, 131.5, 131.4, 130.8, 130.5, 130.2, 129.5, 129.2, 127.8, 127.4, 126.9, 126.7, 126.3, 125.7, 125.3, 125.0, 122.1, 121.8, 66.9, 17.2, 17.0, 14.7, 14.6, 12.5, 12.3, 11.2. ^{11}B NMR ($CDCl_3$, ppm) 0.78. HRMS (p-ESI) calcd. for $C_{52}H_{41}BBr_2F_2N_2$: m/z 902.1677; found: m/z 902.1694.

Monomer F-DPA-BO. Similarly to the preparation of **F-PY-BO**, compound **F-DPA-BO** was prepared from the **3** (4.70 g, 6.20 mmol) and 2,4-dimethyl-3-ethyl-1H-pyrrole (1.53 g, 12.4 mmol) in the absolute dichloromethane (20 mL) with TFA (4 drops), DDQ (1.50 g, 6.60 mmol), triethylamine (12 mL) and $BF_3{\cdot}OEt_2$ (15 mL) in 25% yield as a red solid (1.60 g). ^{1}H NMR ($CDCl_3$, ppm) 7.74−7.66 (m, 3H), 7.62−7.53 (m, 3H), 7.52−7.45 (m, 7H), 7.44−7.39 (m, 4H), 7.35−7.27 (m, 6H), 7.20 (d, *J* = 8.1 Hz, 2H), 7.13 (d, *J* = 8.0 Hz, 2H), 2.51 (s, 6H), 2.29 (q, *J* = 7.3 Hz, 4H), 1.21 (s, 6H), 0.97 (t, *J* = 7.4 Hz, 6H). ^{13}C NMR ($CDCl_3$, ppm) 153.7, 152.5, 145.0, 139.5, 139.4, 138.7, 138.3, 138.0, 137.4, 136.9, 134.8, 132.8, 131.2, 131.0, 130.9, 130.6, 130.1, 129.3, 128.9, 128.6, 128.4, 128.2, 127.8, 127.6, 127.4, 127.0, 125.5, 125.2, 125.0, 121.8, 121.6, 65.5, 17.0, 14.6, 12.5, 11.6. ^{11}B NMR ($CDCl_3$, ppm) 0.78. HRMS (p-APCI) calcd. for $C_{62}H_{49}BBr_2F_2N_2$+H^+: m/z 1031.2376; found: m/z 1031.2355.

Monomer F-PY. Similarly to the preparation of **2**, compound **F-PY** was prepared from **4** (8.00 g, 14.7 mmol) and pyrene (3.27 g, 16.2 mmol) in the presence of trifluoromethanesulfonic acid (3.30 g, 22.0 mmol) and dioxane (55 mL) in 77% yield as a pale yellow solid (8.20 g). ^{1}H NMR ($CDCl_3$, ppm) 8.16 (d, *J* = 8.2, 1H), 8.10 (m, *J* = 7.0, 1H), 8.07−7.93 (m, 5H), 7.87 (br, 1H), 7.75 (br, 3H), 7.63 (d, *J* = 8.2 Hz, 2H), 7.50 (d, *J* = 8.2 Hz, 2H), 7.12 (d, *J* = 6.3 Hz, 2H), 6.79 (d, *J* = 8.2 Hz, 2H), 3.89 (t, *J* = 6.3 Hz, 2H), 1.75 (m, 2H), 1.43 (m, 2H), 1.31 (br, 8H), 0.92 (t, *J* = 6.9 Hz, 3H). ^{13}C NMR ($CDCl_3$, ppm) 158.2, 154.3, 137.7, 137.4, 137.1, 131.3, 131.2, 131.0, 130.2, 129.4, 127.6, 127.3, 126.6, 126.4, 126.0, 125.4, 125.1, 124.8, 124.6, 122.0, 121.7, 114.9, 67.9, 66.2, 31.8, 29.3, 29.2, 26.0, 22.6, 14.1. HRMS (p-APCI) calcd. for $C_{43}H_{36}O+H^+$: m/z 729.1191; found: m/z 729.1178.

Monomer F-DPA. Similarly to the preparation of **2**, compound **F-DPA** was prepared from **4** (3.50 g, 6.43 mmol) and 9,10-diphenylanthracene (2.55 g, 7.72 mmol) in the presence of trifluoromethanesulfonic acid (1.45 g, 9.66 mmol) and dichloromethane (25 mL) in 60% yield as a pale yellow solid (3.30 g). ^{1}H NMR ($CDCl_3$, ppm) 7.70 (m, 3H), 7.59 (m, 2H), 7.54 (d, *J* = 7.6 Hz, 1H), 7.47 (m, 5H), 7.45 (m, 4H), 7.39 (dd, *J* = 8.0 Hz, 2.5 Hz, 2H), 7.33 (m, 2H), 7.29 (m, 3H), 7.23 (m, 1H), 7.01, (d, *J* = 8.3 Hz, 2H), 6.75 (d, *J* = 8.8 Hz, 2H), 3.90 (t, *J* = 7.1 Hz, 2H), 1.75 (m, 2H), 1.44 (m, 2H), 1.31 (m, 8H), 0.90 (t, *J* = 7.1 Hz, 3H). ^{13}C NMR ($CDCl_3$, ppm) 158.3, 152.8, 140.4, 138.8, 138.2, 137.9, 137.4, 136.8, 135.2, 131.3, 130.9, 130.7, 130.9, 130.0, 129.3, 129.2, 129.1, 128.8, 128.4, 128.2, 127.4, 127.0, 126.1, 125.1, 124.7, 121.6, 121.5, 114.5, 68.0, 65.0, 31.8, 29.3, 29.2, 26.0, 22.6, 14.1. HRMS (p-APCI) calcd. for $C_{53}H_{44}Br_2O+H^+$: m/z 857.1811; found: m/z 857.1804.

Polymer PF-PY-BO-TBT. The solution containing **F-PY-BO** (49.3 mg, 55 μmol), benzothiadiazole (43.4 mg, 55 μmol), $Pd_2(dba)_3$ (0.05 mg, 0.5 μmol) and tri(2-furyl)phosphine (1 mg, 4.5 μmol) in 0.5 mL of anhydrous toluene was stirred at 100 °C for 5 days under argon atmosphere. The resulting products were reprecipitated twice with a small amount of chloroform into 50 mL of methanol.

Filtration gave **PF-PY-BO-TBT** as a red solid (65 mg, 94%). ^{1}H NMR ($CDCl_3$, ppm) 8.38 (1H), 8.18 (2H), 8.04 (2H), 7.99 (3H), 7.87 (2H), 7.83 (2H), 7.73 (3H), 7.55 (2H), 7.42 (2H), 7.18 (2H), 7.14 (2H), 2.57 (4H), 2.51 (3H), 2.45 (3H), 2.36 (2H), 2.16 (2H), 1.68 (3H), 1.18 (7H), 1.14 (12H), 1.04 (3H), 0.77 (9H). ^{13}C NMR ($CDCl_3$, ppm) 154.1, 153.7, 152.7, 144.6, 142.9, 139.1, 138.4, 134.3, 132.8, 131.9, 131.5, 130.8, 130.4, 129.5, 129.0, 127.5, 126.7, 125.9, 125.5, 125.1, 123.7, 121.8, 120.9, 66.8, 31.5, 30.6, 29.5, 29.1, 22.5, 17.0, 14.7, 14.5, 14.0, 12.4, 11.5. ^{11}B NMR ($CDCl_3$, ppm) 0.78.

Polymer PF-DPA-BO-TBT. Similarly to the preparation of **PF-PY-BO-TBT**, **PF-DPA-BO-TBT** was prepared from **F-DPA-BO** (103.7 mg, 100 μmol) and benzothiadiazole (79.4 mg, 100 μmol) in the presence of $Pd_2(dba)_3$ (1 mg, 1 μmol), tri(2-furyl)phosphine (2 mg, 9 μmol) and anhydrous toluene (1 mL) in 97% yield as a red solid (130 mg). ^{1}H NMR ($CDCl_3$, ppm) 7.74 (1H), 7.69 (7H), 7.59 (4H), 7.53 (2H), 7.47 (3H), 7.41 (2H), 7.33 (3H), 7.31 (5H), 7.23 (2H), 7.13 (2H), 2.70 (4H), 2.49 (6H), 2.26 (4H), 1.68 (3H), 1.29 (4H), 1.22 (12H), 1.20 (3H), 0.93 (6H), 0.81 (6H). ^{13}C NMR ($CDCl_3$, ppm) 154.2, 153.7, 153.6, 152.0, 146.1, 145.6, 144.8, 142.9, 140.4, 140.0, 139.3, 138.9, 138.7, 138.4, 137.4, 136.8, 134.4, 133.9, 132.8, 132.7, 131.8, 131.3, 131.0, 130.7, 130.2, 129.7, 129.5, 129.0, 128.9, 128.7, 128.6, 128.5, 128.4, 128.2, 127.5, 127.4, 127.0, 126.0, 125.8, 125.6, 125.4, 125.2, 123.1, 121.6, 120.7, 65.6, 31.6, 31.0, 30.8, 29.7, 29.2, 22.6, 17.1, 14.6, 14.0, 12.5, 11.8, 11.7. ^{11}B NMR ($CDCl_3$, ppm) 0.78.

Polymer PF-PY-TBT. Similarly to the preparation of **PF-PY-BO-TBT**, **PF-PY-TBT** was prepared from **F-PY** (73.0 mg, 100 μmol) and benzothiadiazole (79.4 mg, 100 μmol) in the presence of $Pd_2(dba)_3$ (1 mg, 1 μmol), tri(2-furyl)phosphine (2 mg, 9 μmol) and anhydrous toluene (1 mL) in 94% yield as a red solid (97 mg). ^{1}H NMR ($CDCl_3$, ppm) 8.14 (1H), 8.07 (1H), 8.04 (2H), 7.95 (3H), 7.83 (4H), 7.69 (4H), 7.53 (3H), 7.15 (3H), 6.78 (2H), 3.90 (2H), 2.56 (4H), 1.74 (2H), 1.54 (4H), 1.42 (2H), 1.26 (8H), 1.14 (12H), 0.85 (3H), 0.77 (6H). ^{13}C NMR ($CDCl_3$, ppm) 158.1, 158.0, 154.0, 144.7, 142.8, 138.9, 138.4, 138.2, 137.5, 133.9, 131.9, 131.7, 131.4, 131.1, 131.0, 130.4, 130.3, 129.7, 129.5, 127.4, 127.1,

126.3, 126.0, 125.4, 125.2, 125.1, 125.0, 124.7, 123.5, 121.7, 121.6, 120.8, 114.8, 68.0, 66.2, 31.8, 31.5, 30.8, 30.6, 29.5, 29.3, 29.2, 29.1, 26.1, 22.6, 22.5, 14.1, 14.0.

Polymer PF-DPA-TBT. Similarly to the preparation of **PF-PY-BO-TBT**, **PF-DPA-TBT** was prepared from **F-DPA** (92.0 mg, 107 μmol) and benzothiadiazole (85.3 mg, 107 μmol) in the presence of $Pd_2(dba)_3$ (1 mg, 1 μmol), tri(2-furyl)phosphine (2 mg, 9 μmol) and anhydrous toluene (1 mL) in 92% yield as a red solid (115 mg). ^{1}H NMR ($CDCl_3$, ppm) 7.65 (7H), 7.57 (5H), 7.44 (7H), 7.23 (7H), 7.04 (3H), 6.72 (2H), 3.87 (2H), 2.66 (4H), 1.64 (6H), 1.38 (2H), 1.25 (8H), 1.20 (12H), 0.80 (9H). ^{13}C NMR ($CDCl_3$, ppm) 158.1, 158.0, 154.3, 154.1, 153.2, 152.0, 151.6, 144.8, 142.9, 142.7, 141.5, 140.9, 138.9, 138.5, 138.3, 137.6, 137.4, 136.7, 135.8, 134.0, 133.6, 131.9, 131.3, 130.9, 130.6, 130.0, 129.6, 129.4, 129.1, 128.8, 128.3, 128.1, 127.9, 127.4, 127.2, 127.0, 126.3, 125.5, 125.3, 124.94, 124.87, 123.1, 121.4, 120.6, 144.4, 67.9, 64.9, 31.8, 31.5, 30.8, 30.7, 30.6, 29.7, 29.31, 29.25, 29.21, 29.2, 26.0, 22.6, 22.5, 14.1, 14.0.

Results and discussion

Synthesis. Three kinds of the dyes were used in this study. The polymer main-chain was composed of the alternating sequence with fluorene and dithiophenylbenzothiadiazole (TBT). These alternating polymers are known as a class of low-band gap polymers for fabricating organic opto-electric devices such as photovoltaic cells and electroluminescence displays and showed the emission in the red region originated from the intramolecular charge transfer (CT) state ($\lambda_{em,max}$ = 625 nm).[22–26] As a blue emissive unit, pyrene and DPA were introduced at the cardo carbon. The BODIPY unit was also tethered to the polymer as a green fluorescent unit.[27–31] The sharp and intense emissions are favorable to modulate the energy transfer to the TBT unit.[16] Modified fluorenes with different types of dyes were synthesized according to Scheme 1 using 2,7-dibromo-9H-fluoren-9-ol derivatives as a starting material. All monomers were characterized by ^{1}H, ^{13}C and ^{11}B NMR spectroscopies and mass measurements.

Scheme 1

The polymerizations with a series of the fluorene monomers **F-PY-BO**, **F-DPA-BO**, **F-PY**, **F-DPA**, **F-BO**, and 2,7-dibromo-9,9-didodecylfluorene were performed with the TBT comonomer via a Stille coupling reaction (Scheme 2). The polymer properties are shown in Table 1. The polymers were obtained as red solids in good yields (91–100%). The number-average molecular weights (M_n) and the molecular weight distributions (M_w/M_n) of the polymers, measured by the size-exclusion chromatography (SEC) in chloroform toward polystyrene standards were from 12,000 to 17,000 with 1.6 to 3.1, respectively (the profiles are shown in Figure S6 in the Supporting Information). The degrees of polymerization (DP) of the polymers were suppressed in the range of 24−31 by regulating the reaction time for maintaining the solubility in the common organic solvents such as THF and chloroform. The

data for structural analysis by ^{1}H, ^{13}C and ^{11}B NMR were corresponded to those of the monomers. Thus, we concluded that the polymers should possess the designed chemical structures.

Scheme 2 and Table 1

Absorption properties. To investigate the electronic interaction involving the dye units and the polymer main-chain at the ground state, the optical properties of the compounds were measured. Initially, the absorption spectra of the monomers **F-PY-BO** and **F-DPA-BO** were monitored in chloroform solution (Figure 1). The results from the measurements are summarized in Table 2. Pyrene and DPA showed well-resolved vibration structures and absorption peaks in the regions of 260−340 nm and 330−400 nm in the spectra, respectively. **F-PY-BO** and **F-DPA-BO** presented vibration structures with similar patterns in the wavelength regions of 250–360 nm and 330–410 nm in the spectra, respectively. Both compounds also exhibited the absorption bands around 450–500 nm originated from the BODIPY unit. Peak shifts of the absorption bands were hardly observed. These data indicate that the electronic structures of the dye units should be hardly perturbed by linking via the cardo carbon.

Figure 1 and Table 2

Next, the absorption spectra with the polymers were examined. All measurements were performed with the concentration of 1.0×10^{-5} M to a polymer repeat unit. Similarly to those of the monomers, a sum of the spectra from each component was obtained. Although slight broadening occurred, the vibrational structures of pyrene and DPA and the absorption band of the BODIPY unit were obviously obtained from the polymers. In addition, the broad absorption bands with the peak around 470 nm

attributed from the polymer main-chain were observed. These data indicate that the electronic interaction between the dyes and the polymer main-chain should hardly occur. The absorption spectra of the polymers were observed in the film states (Figure 2, Table 3). The thin films with the thickness of approximately 100 nm for the measurements were prepared by the spin-coating method with the chloroform solutions (1.0 mg/mL) of the polymers on the quartz plate. The absorption spectra in the film states of the polymers exhibited similar shapes to those from solution states. These data propose that the cardo structure could contribute to the preservation of the electronic states even in the condensed states.

Figure 2 and Table 3

Energy transfer from the blue dyes to BODIPY linked via the cardo carbon. The energy transfer efficiencies were calculated by the following equation (1).[16]

$$E_{eff} = 1 - (I_{DA}/A_{DA}) / (I_D/A_D) \qquad (1)$$

where I_{DA} is a fluorescence intensity of donor (pyrene, DPA, or BODIPY) in the presence of acceptor (the polymer main-chains) and I_D in the absence of acceptor. A_{DA} is an absorption of donor in the presence of acceptor and A_D in the absence of acceptor. The absorptions were determined from the subtraction of the spectra. The energy transfer efficiencies were calculated from the ratio of the emission intensities (Table 2). With the chloroform solutions of **F-PY-BO** and **F-DPA-BO**, the photoluminescence spectra were measured with the excitation light at each of absorption maxima of blue dyes (Figure 3). **F-PY-BO** showed a green emission band with the peak at 540 nm. **F-DPA-BO** exhibited a dual emission with a weak emission band in the region between 400 nm and 500 nm and a strong emission band in the green region. These data clearly indicate that dual-emissive properties can be modulated by selecting the energy donor molecule. These data also mean that the energy transfer should be varied by changing the donors in the side chains. According to the energy transfer efficiencies

summarized in Table 2, it was found that both proceed effectively (from pyrene, 95%; DPA, 96%; calculated by intensities). Moreover, the energy transfer was examined by monitoring excitation spectra detected in the green region (Figure S1). The excitation spectra showed good agreements with well-resolved vibration structures of pyrene and DPA observed in the absorption spectra. These results mean that the green emission can be generated by the absorption of blue light. It is suggested that the excitation energy can migrate efficiently between the side chains.

Figure 3

Energy transfer efficiency from the blue dyes to the red-emissive polymer main-chains. Next, the energy transfer efficiencies from the blue emissive dyes (pyrene or DPA) to the polymer main-chain having the red emission were investigated in the chloroform solution (Table 2). The photoluminescence spectra were monitored with the excitation light at the absorption maxima of the blue-emissive component (Figure 4). Interestingly, the different transfer efficiencies were obtained from the polymers. **PF-PY-TBT** exhibited dual emission peaks in the region of 350−450 nm and 550−700 nm. The efficiency was approximately 80%. In contrast, **PF-DPA-TBT** showed a broad emission band with the peak around 620 nm attributable to the emission from the polymer main-chain. Energy transfer in **PF-DPA-TBT** proceeded with high efficiency (99%). The energy transfer was also confirmed in excitation spectra detected in the emission region of the polymer main-chain (Figure S2). It was shown that the excitation energy in **PF-DPA-TBT** was quantitatively transferred to the polymer main-chain. These data indicate that the energy transfer efficiency can be modulated by selecting the blue-emissive unit, resulting in the monotonous strong emission or the dual emission. Interestedly, although the overlap of the spectra between the emission of pyrene and the absorption of the polymer main-chain should be smaller than that of DPA, the insufficient energy transfer was observed in **PF-PY-TBT** comparing to

that in **PF-DPA-TBT**. There is possibility that the transient dipole moment in the pyrene unit might have an unfavorable direction, leading to the decrease of the energy transfer efficiency.[32] Because of the connection to the cardo fluorene, it should be intrinsically difficult to form the parallel distribution toward the transition moment of the main-chain conjugation. In addition, due to the steric hindrance, the molecular motion of the pyrene unit could be inhibited. Thereby, it is implied that the energy transfer might be suppressed via the cardo structure.

Figure 4

Energy transfer with the blue-green-red system. The energy transfer was examined with the polymers having the RGB-color units (**PF-PY-BO-TBT** and **PF-DPA-BO-TBT**). With the chloroform solutions containing each polymer, the photoluminescence spectra were recorded with the excitation light at each of absorption maxima of the blue-emissive units (Figure 5). Both polymers showed slight emissions in the blue regions. The energy transfer from the blue to green units and from the blue to red units occurred efficiently (>99%). The kinetic data proposed the rational results (Table 4). The lifetimes of both blue-emissive units were relatively shorter than those of free molecules. The excitation spectra were measured with the detection wavelength at 628 nm (Figure S3). The peak positions showed good agreements with those in absorption spectra. These results indicate that the red emission should be induced via the blue-emissive dyes and the BODIPY unit. These results clearly indicate that the energy transfers from the blue-emissive units should proceed with high efficiency. In contrast, from the green to red units, the energy transfer proceeds insufficiently, resulting in the multi-emission behaviors. The apparent energy transfer efficiencies from the BODIPY units to the polymer main-chains were 8.3% and 39% in **PF-PY-BO-TBT** and **PF-DPA-BO-TBT**, respectively. Because of the relationships of the energy levels of each unit, the energy transfer should be disturbed.[16] These results can be summarized

that the energy transfer efficiencies should be controllable by regulating the energy levels of the dye units.

Figure 5 and Table 4

Dual-emission properties in the film state. From above results in the solution states, it was revealed that the **PF-PY-BO-TBT** and **PF-DPA-BO-TBT** showed dual emission of green and red color derived from the BODIPY unit and the polymer main-chain, respectively. In the previous report, the dual emission was also observed from the BODIPY-tethered alternating fluorene copolymer with TBT only in the solution state.[16] Finally, to evaluate the dual-emissive properties of the polymers in the film state, the optical measurements were performed. The homogeneous films (ca. 100 nm) of the synthesized polymers were prepared on the quartz by the spin-coating method with the chloroform solutions (1.0 mg/mL). From the microscopic observations, it was confirmed that all polymer films possess homogeneous states at the sub-micron order (Figure S4). From the fluorescence measurements, the dual emissions were observed from the films of **PF-PY-BO-TBT** and **PF-DPA-BO-TBT** (Figure 6). The significant emission bands in the blue regions from 400 nm to 500 nm and the red regions around 600 nm were simultaneously obtained. These data clearly indicate that the dye-modified alternating polymers can work as a dual-emissive materials in the film state. The quantum yields in the film state were lower than those in the solution (Tables 2 and 3). The excitation spectra were measured with the detection wavelength at 625nm (Figure S5). The similar spectra were obtained to those in absorption spectra (Figure 2). These data mean that the energy transfers could proceed. The decreases of the emission in the films could be caused by the inter-chain electronic interaction in the condensed state. Since the emission from the BODIPY unit can be critically quenched in the film state, even on the cardo structure, concentration quenching could occur in the BODIPY-containing polymers **PF-PY-BO-TBT** and **PF-**

DPA-BO-TBT (Φ_{PL} = 0.08), leading to the decreases of the quantum yields comparing to those of **PF-PY-TBT** and **PF-DPA-TBT** (Φ_{PL} > 0.2).

Figure 6

Conclusion

We present the dual-emissive solid materials based on the alternating polymers composed of different dyes-substituted cardo fluorenes. We also demonstrate the systematic information on the energy transfer in the dyes-substituted cardo fluorenes involving the polymer main-chains. According to the experimental results, three significant issues are obtained: i) The efficient energy transfer can occur between the side chains and from the side chain to the main chain. In this study, the energy transfers from the blue-emissive dyes tethered to the cardo structure to the green and red-emissive components in the polymers are shown. ii) The energy transfer efficiencies are controllable by modulating the energy levels of the donor and the acceptor and by changing the detection conditions such in the solution or film. iii) The dual emission can be observed even from the homogeneous polymer films. Insufficient energy transfer was accomplished, leading to the dual emission. In particular, it is illustrated that the cardo structures play a crucial role in the isolation of the electronic states of each emissive component. Our findings described here could be feasible for constructing multi-functional optical assembly using fluorene-based polymers as a scaffold to receive advanced opto and/or electronic materials.

Acknowledgement

This work was partially supported by the Tokuyama Science Foundation (for K.T.), "the Adaptable and Seamless Technology Transfer Program" through target-driven R&D, Japan Science and Technology Agency (JST) and a Grant-in-Aid for Scientific Research on Innovative Areas “New Polymeric Materials Based on Element-Blocks (No.2401)” (24102013) of The Ministry of Education, Culture, Sports, Science, and Technology, Japan.

REFERENCES

1. Chong, H.; Nie, C.; Zhu, C.; Yang, Q.; Liu, L.; Lv, F.; Wang, S. *Langmuir* **2012**, *28*, 2091−2098.

2. Wang, H.-Y.; Qian, Q.; Lin, K.-H.; Peng, B.; Huang, W.; Liu, F.; Wei, W. *J. Polym. Sci. Part A: Polym. Chem*. **2012**, *50*, 180–188.

3. Takamizu, K.; Inagaki, A.; Nomura, K. *ACS Macro Lett*. **2013**, *2*, 980−984.

4. Kuo, C.-P.; Chuang, C.-N.; Chang, C.-L.; Leung, M.; Lian, H.-Y.; Wu, K. C.-W. *J. Mater. Chem. C* **2013**, *1*, 2121−2130.

5. Lin, J-Y.; Wong, J.; Xie, L.-H.; Dong, X.-C.; Yang, H. Y.; Huang, W. *Macromol. Rapid Commun*. **2014**, *35*, 895−900.

6. Osken, I.; Gundogan, A. S.; Tekin, E.; Eroglu, M. S.; Ozturk, T. *Macromolecules* **2013**, *46*, 9202−9210.

7. Luo, J.; Li, X.; Chen, J.; Huang, F.; Cao, Y. *Syn. Met*. **2011**, *161*, 1982−1986.

8. Tanaka, K.; Tamashima, K.; Nagai, A.; Okawa, T.; Chujo, Y. *Macromolecules* **2013**, *46*, 2969–2975.

9. Yoshii, R.; Hirose, A.; Tanaka, K.; Chujo, Y. *J. Am. Chem. Soc*. **2014**, *136*, 18131−18139.

10. Yoshii, R.; Tanaka, K.; Chujo, Y. *Macromolecules* **2014**, *47*, 2268−2278.

11. Yoshii, R.; Nagai, A.; Tanaka, K.; Chujo, Y. *Macromol. Rapid Commun*. **2014**, *35*, 1315−1319.

12. Yu, J.; Zheng, Y.; Huang, J. *Polymers* **2014**, *6*, 2473−2509.

13. Pei, J.; Wen, S.; Zhou, Y.; Dong, Q.; Liu, Z.; Zhang, J.; Tian, W. *New J. Chem*. **2011**, *35*, 385−393.

14. Yeo, H.; Tanaka, K.; Chujo, Y. *J. Polym. Sci. Part A: Polym. Chem*. **2012**, *50*, 4433–4442.

15. Yeo, H.; Tanaka, K.; Chujo, Y. *Macromolecules* **2013**, *46*, 2599–2605.

16. Yeo, H.; Tanaka, K.; Chujo, Y. *Polymer* **2015**, DOI:10.1016/j.polymer.2015.01.056.

17. Wu, H.; Ying, L.; Yang, W.; Cao, Y. *Chem. Soc. Rev*. **2009**, *38*, 3391−3400.

18. Bu, J.; Watanabe, K.; Hayasaka, H.; Akagi, K. *Nat. Commun*. **2014**, *5*, DOI: 10.1038/ncomms4799.

19. Palmer, G. M.; Fontanella, A. N.; Zhang, G.; Hanna, G.; Fraser, C. L.; Dewhirst, M. W. *J. Biomed. Opt*. **2010**, *15*, 066021.

20. Zhang, G.; Palmer, G. M.; Dewhirst, M. W.; Fraser, C. L. *Nat. Mater*. **2009**, *8*, 747–751.

21. Okamoto, A.; Tainaka, K.; Nishiza, K.; Saito, I. *J. Am. Chem. Soc*. **2005**, *127*, 13128–13129.

22. Svensson, M.; Zhang, F.; Veenstra, S. C.; Verhees, W. J. H.; Hummelen, J. C.; Kroon, J. M.; Inganäs, O.; Andersson, M. R. *Adv. Mater*. **2003**, *15*, 988−991.

23. Edder, C.; Armstrong, P. B.; Prado, K. B.; Fréchet, J. M. J. *Chem. Commun*. **2006**, 1965−1967.

24. Akhtaruzzaman, M.; Tomura, M.; Nishida, J.; Yamashita, Y. *J. Am. Chem. Soc*. **1995**, *117*, 6791−6792.

25. Mullekom, H. A. M. V.; Vekemans, J. A. J. M.; Meijer, E. W. *Chem.−Eur. J*. **1998**, *4*, 1235−1243.

26. Martinelli, C.; Farinola, G. M.; Pinto, V.; Cardone, A. *Materials* **2013**, *6*, 1205−1236.

27. Ooyama, Y.; Hagiwara, Y.; Oda, Y.; Fukuoka, H.; Ohshita, J. *RSC Adv*. **2014**, *4*, 1163−1167.

28. Yoshii, R.; Yamane, H.; Tanaka, K.; Chujo, Y. *Macromolecules* **2014**, *47*, 3755−3760.

29. Yoshii, R.; Yamane, H.; Nagai, A.; Tanaka, K.; Taka, H.; Kita, H.; Chujo, Y. *Macromolecules* **2014**, *47*, 2316−2323.

30. Tanaka, K.; Yamane, H.; Yoshii, R.; Chujo, Y. *Bioorg. Med. Chem*. **2013**, *21*, 2715–2719.

31. Yoshii, R.; Nagai, A.; Tanaka, K.; Chujo, Y. *J. Polym. Sci. Part A: Polym. Chem.* **2013**, *51*, 1726–1733.

32. Morisaki, Y.; Kawakami, N.; Nakano, T.; Chujo Y. *Chem.−Eur. J.* **2013**, *19*, 17715−17718.

Table 1. Polymerization results

Polymers	Yield (%)[a]	M_n[b]	M_w/M_n[b]	DP[c]
PF-PY-BO-TBT	94	16,000	3.09	26
PF-DPA-BO-TBT	97	16,000	2.03	24
PF-PY-TBT	94	16,000	2.18	31
PF-DPA-TBT	92	17,000	1.94	28
PF-BO-TBT	91	17,000	1.85	28
PF-TBT	~100	12,000	1.64	24

[a] Isolated yields after precipitation.

[b] Estimated by size-exclusion chromatography (SEC) based on polystyrene standards in chloroform.

[c] Degree of polymerization estimated by number-average molecular weight.

Table 2. Photophysical properties of the polymers in solution state

Compound	$\lambda_{abs,max}$ / nm[a]	$\lambda_{PL,max}$ / nm[b]	Φ_{PL}[c]	Φ_{DA}[d]	η_{ET}[e]
BODIPY	378, 527	537[f]	0.68[g]	–	–
Pyrene	275, 322, 338	373, 393[h]	0.32[h]	–	–
DPA	262, 376, 396	410, 431[g]	0.95[g]	–	–
F-PY-BO	280, 335, 352, 528	537[h]	0.97[h]	0.002[h]	0.945
F-DPA-BO	274, 377, 398, 527	537[g]	0.56[g]	0.02[g]	0.962
PF-PY-BO-TBT	336, 353, 527	538, 620[h]	0.66[h]	0.003[h]	0.931[i], 0.083[j]
PF-DPA-BO-TBT	273, 373, 527	537, 617[g]	0.48[g]	0.001[g]	0.995[i], 0.385[j]
PF-PY-TBT	336, 353, 467	401, 620[h]	0.58[h]	0.002[h]	0.799
PF-DPA-TBT	272, 364, 467	618[g]	0.44[g]	0.001[g]	0.993
PF-BO-TBT	368, 527	539, 625[f]	0.37[k]	–	0.936
PF-TBT	368, 467	624[k]	0.39[k]	–	–

[a] Evaluated in chloroform (1.0×10^{-5} M).

[b] Evaluated in chloroform (1.0×10^{-7} M).

[c] Absolute quantum yield.

[d] Absolute quantum yield of the pyrene or DPA.

[e] Energy transfer efficiency calculated by emission intensity (from pyrene or DPA to BODIPY and polymer main-chain).

[f] Excited at 525 nm in chloroform (1.0×10^{-7} M).

[g] Excited at 376 nm in chloroform (1.0×10^{-7} M).

[h] Excited at 338 nm in chloroform (1.0×10^{-7} M).

[i] Apparent energy transfer efficiency (from pyrene or DPA to BODIPY and polymer main-chain).

[j] Apparent energy transfer efficiency (from BODIPY to polymer main-chain).

[k] Excited at 467 nm in chloroform (1.0×10^{-7} M).

Table 3. Photophysical properties of the polymers in film states

Compound	$\lambda_{abs,max}$ / nm [a]	$\lambda_{PL,max}$ / nm [b]	Φ_{PL} [c]
PF-PY-BO-TBT	353, 533	623	0.08
PF-DPA-BO-TBT	372, 533	620	0.08
PF-PY-TBT	353, 473	621	0.20
PF-DPA-TBT	369, 473	614	0.26

[a] Absorption peak top.

[b] Excited at 465 nm.

[c] Absolute quantum yield.

Table 4. Photoluminescence lifetimes

Compound	τ / ns, 393 nm[a]	χ	τ / ns, 410 nm[b]	χ	τ / ns, 540 nm[c]	τ / ns	τ / ns, 630 nm[d]	χ
BODIPY	–		–		4.99	1.013	–	
DPA	–		4.17	1.193	–		–	
Pyrene	0.827	1.160	–		–		–	
F-PY-BO	5.22	1.090	–		5.91	1.037	–	
F-DPA-BO	–		5.38	1.191	5.72	1.129	–	
PF-PY-BO-TBT	0.647	1.132	–		3.21	1.085	3.36	1.186
PF-DPA-BO-TBT	–		1.61	1.108	4.34	1.161	3.09	1.160
PF-PY-TBT	1.15	1.184	–		–		3.43	1.057
PF-DPA-TBT	–		3.95	1.178	–		3.78	1.153
PF-BO-TBT	–		–		3.28	1.190	2.82	1.162
PF-TBT	–		–		–		3.42	1.129

[a] Emission maxima of pyrene. Evaluated in chloroform (1.0×10^{-7} M).

[b] Emission maxima of DPA. Evaluated in chloroform (1.0×10^{-7} M).

[c] Emission maxima of BODIPY. Evaluated in chloroform (1.0×10^{-7} M).

[d] Emission maxima of polymer main-chain. Evaluated in chloroform (1.0×10^{-7} M).

Scheme 1. Synthesis of the monomers

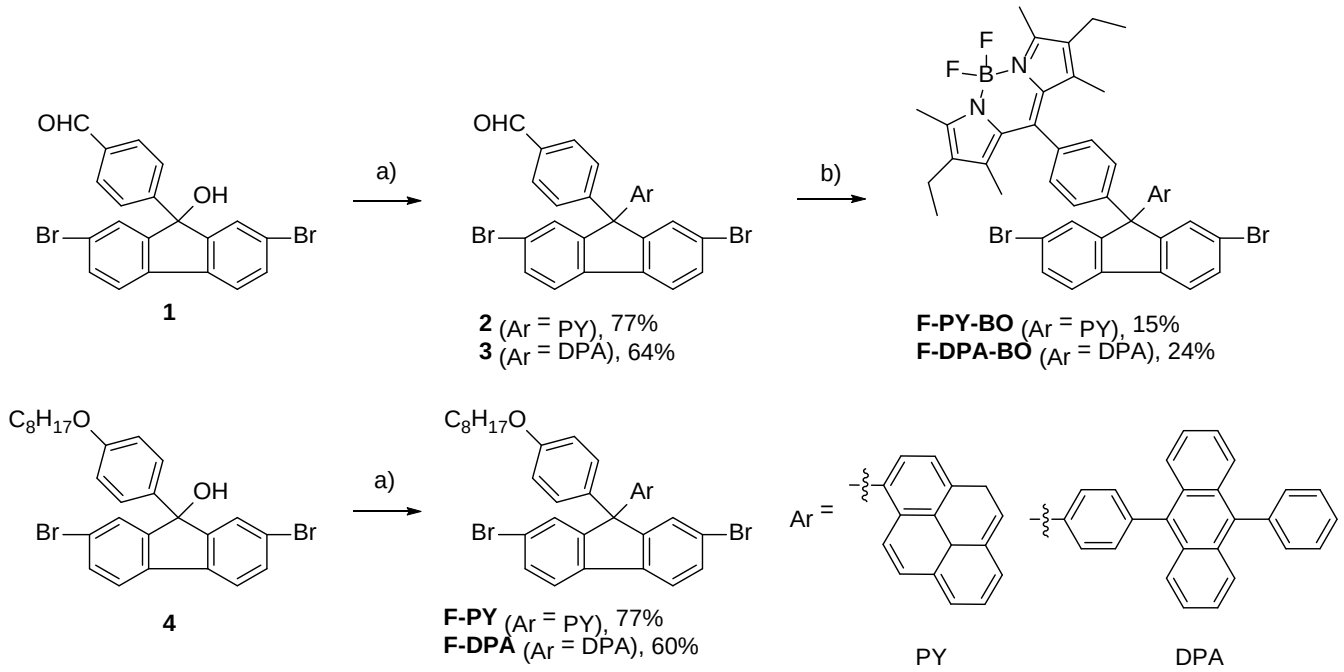

Reagents and conditions: a) Pyrene or 9,10-diphenylanthracene, CF_3SO_3H, in dioxane, 70 °C, 4 h; b) 2,4-dimethyl-3-ethyl-1H-pyrrole, TFA, in CH_2Cl_2, r.t., 3 h.

Scheme 2. Synthesis of the polymers

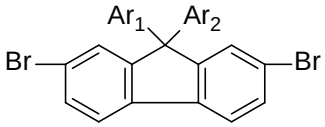

F-PY-BO (Ar_1 = Pyrene, Ar_2 = BODIPY)
F-DPA-BO (Ar_1 = DPA, Ar_2 = BODIPY)
F-PY (Ar_1 = Pyrene, Ar_2 = 4-octoxyphenyl)
F-DPA (Ar_1 = DPA, Ar_2 = 4-octoxyphenyl)
F-BO (Ar_1 = BODIPY, Ar_2 = 4-octoxyphenyl)
2,7-dibromo-9,9-didodecylfluorene (Ar_1, Ar_2 = n-$C_{12}H_{25}$)

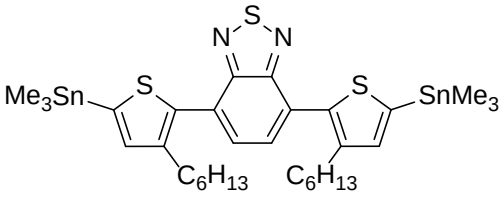

TBT

a)

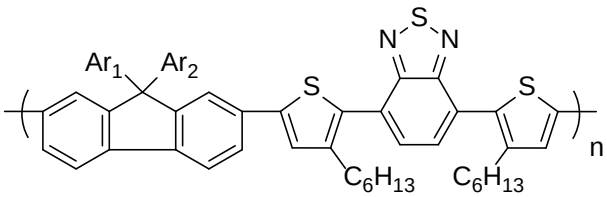

PF-PY-BO-TBT (Ar_1 = Pyrene, Ar_2 = BODIPY), 94%
PF-DPA-BO-TBT (Ar_1 = DPA, Ar_2 = BODIPY), 97%
PF-PY-TBT (Ar_1 = Pyrene, Ar_2 = 4-octoxyphenyl), 94%
PF-DPA-TBT (Ar_1 = DPA, Ar_2 = 4-octoxyphenyl), 92%
PF-BO-TBT (Ar_1 = BODIPY, Ar_2 = 4-octoxyphenyl), 92%
PF-TBT (Ar_1, Ar_2 = $C_{12}H_{25}$), 99%

Ar =

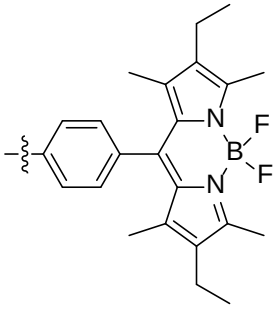

BO

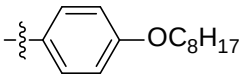

4-octoxyphenyl

Reagents and conditions: a) $Pd_2(dba)_3$, tri(2-furyl)phosphine, toluene, 100 °C, 5 d.

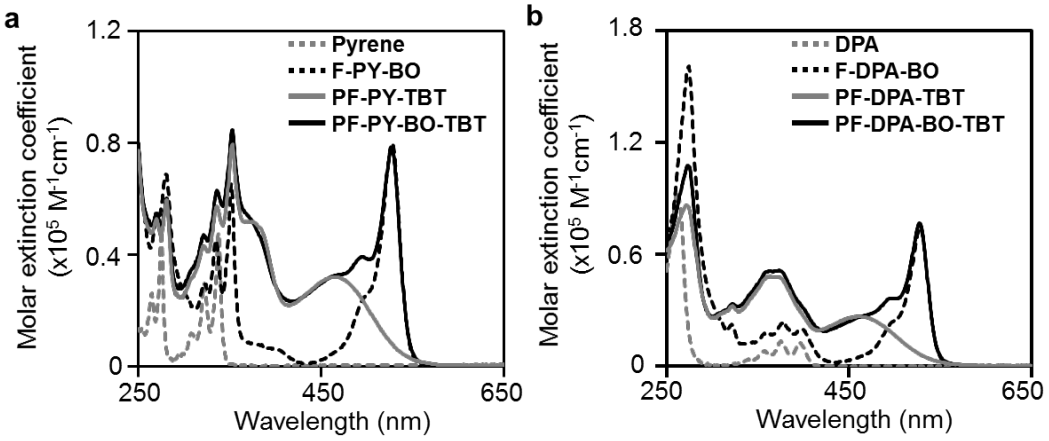

Figure 1. UV−vis spectra of (a) pyrene and (b) DPA derivatives in chloroform (1.0×10^{-5} M).

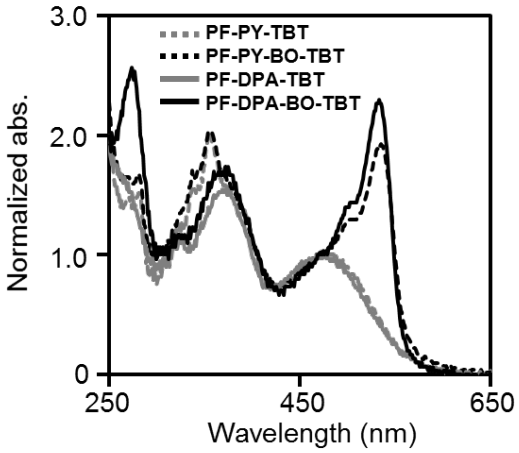

Figure 2. Normalized (465 nm) absorption spectra of the polymers in the film states. The thin films for the measurements were prepared by the spin-coating method with the chloroform solutions (1.0 g/L) of the polymers on the quartz plate.

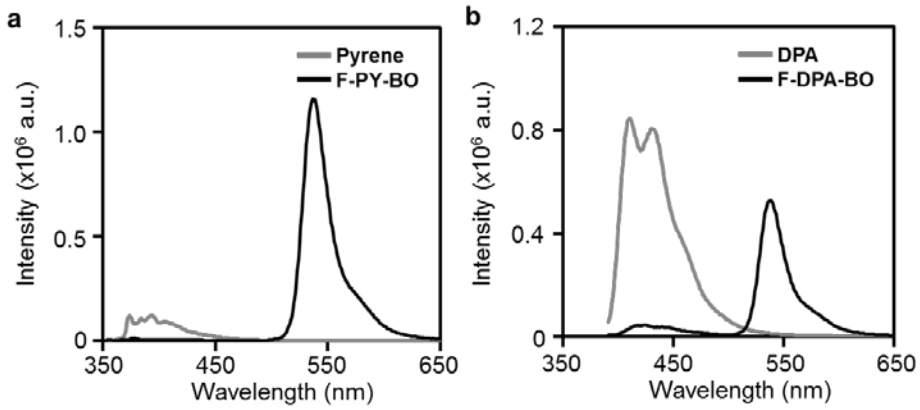

Figure 3. Energy transfer from the blue-emissive dyes to BODIPY unit. (a) Photoluminescence spectra of pyrene and **F-PY-BO** in $CHCl_3$ (1.0×10^{-7} M, excitation wavelength 338 nm). (b) Photoluminescence spectra of DPA and **F-DPA-BO** in $CHCl_3$ (1.0×10^{-7} M, excitation wavelength 376 nm).

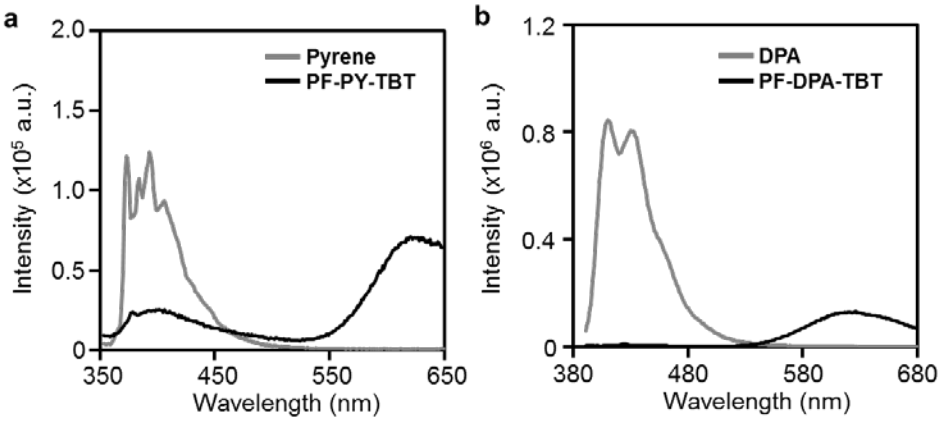

Figure 4. Energy transfer from the blue-emissive dyes to polymer main-chain. (a) Photoluminescence spectra of pyrene and **PF-PY-TBT** in $CHCl_3$ (1.0×10^{-7} M, excitation wavelength 338 nm). (b) Photoluminescence spectra of DPA and **PF-DPA-TBT** in $CHCl_3$ (1.0×10^{-7} M, excitation wavelength 376 nm).

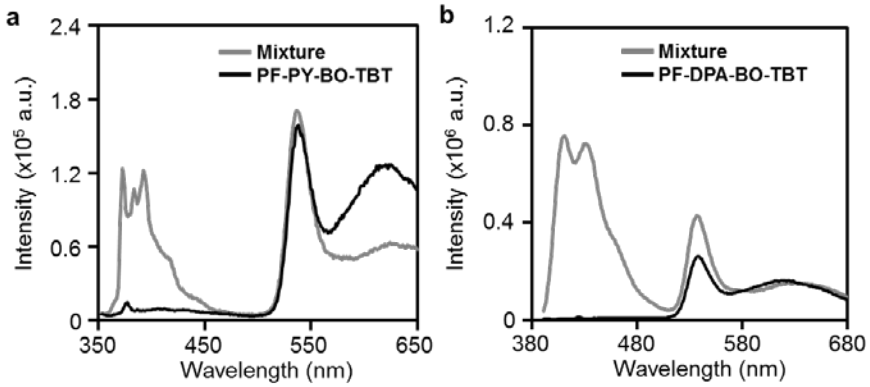

Figure 5. (a) Photoluminescence spectra of the mixture (pyrene, BODIPY and **PF-TBT**) and **PF-PY-BO-TBT** in $CHCl_3$ (1.0×10^{-7} M, excitation wavelength 338 nm) and (b) the mixture (DPA, BODIPY and **PF-TBT**) and **PF-DPA-BO-TBT** in $CHCl_3$ (1.0×10^{-7} M, excitation wavelength 376 nm).

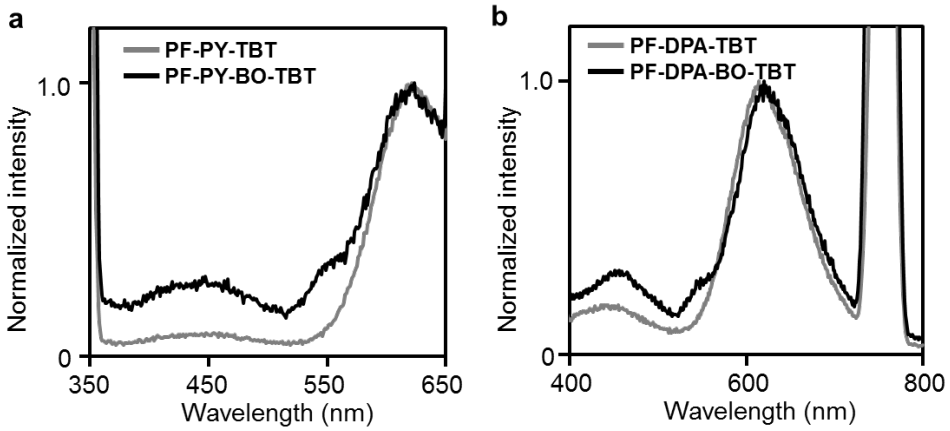

Figure 6. Normalized photoluminescence spectra of the polymers in film states. (a) Excitation wavelength was at 338 nm. (b) Excitation wavelength was at 376 nm.

Supporting Information

Energy Transfer through Heterogeneous Dyes-Substituted Fluorene-Containing Alternating Copolymers and Their Dual-Emission Properties in the Films

Hyeonuk Yeo, Kazuo Tanaka*, Yoshiki Chujo*

Department of Polymer Chemistry, Graduate School of Engineering, Kyoto University, Katsura, Nishikyo-ku, Kyoto 615-8510, Japan

Phone: +81-75-383-2604

Fax: +81-75-383-2605

*To whom correspondence should be addressed: chujo@chujo.synchem.kyoto-u.ac.jp

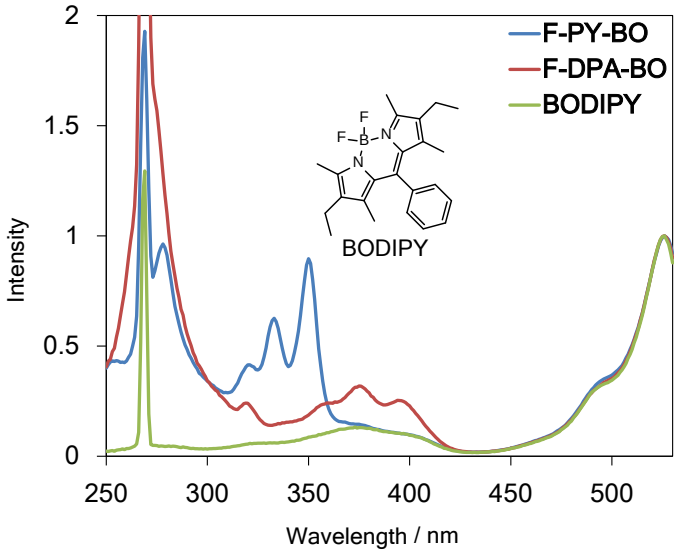

Figure S1. Normalized excitation spectra of **F-PY-BO**, **F-DPA-BO** and BODIPY in $CHCl_3$ (1.0×10^{-7} M, detection wavelength: 540 nm).

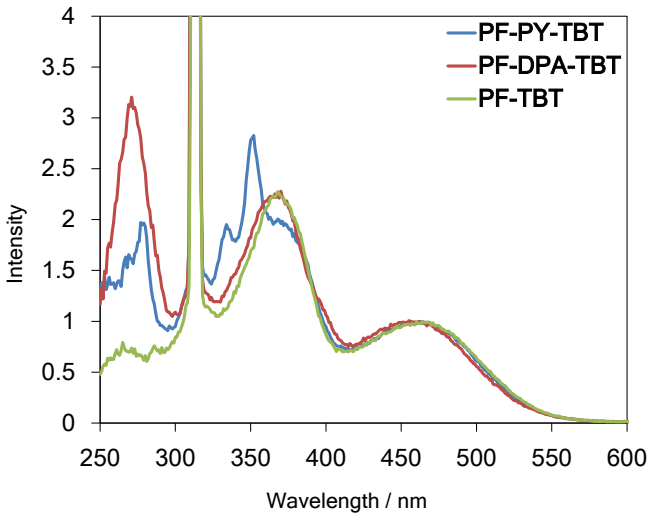

Figure S2. Normalized excitation spectra of **PF-PY-TBT**, **PF-DPA-TBT** and **PF-TBT** in $CHCl_3$ (1.0×10^{-7} M, detection wavelength: 628 nm).

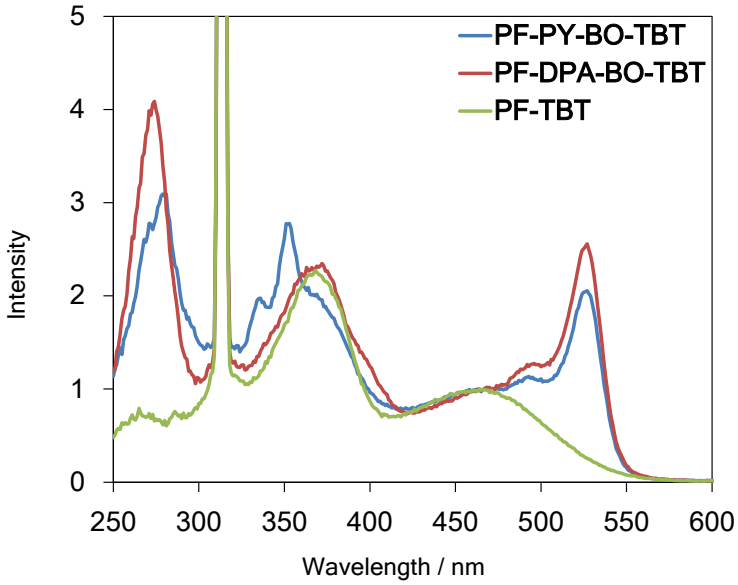

Figure S3. Normalized excitation spectra of **PF-PY-BO-TBT**, **PF-DPA-BO-TBT** and **PF-TBT** in $CHCl_3$ (1.0×10^{-7} M, detection wavelength: 628 nm).

Figure S4. SEM observations of the cast films of (a) **PF-TBT**, (b) **PF-PY-BO-TBT** and (c) **PF-DPA-BO-TBT**.

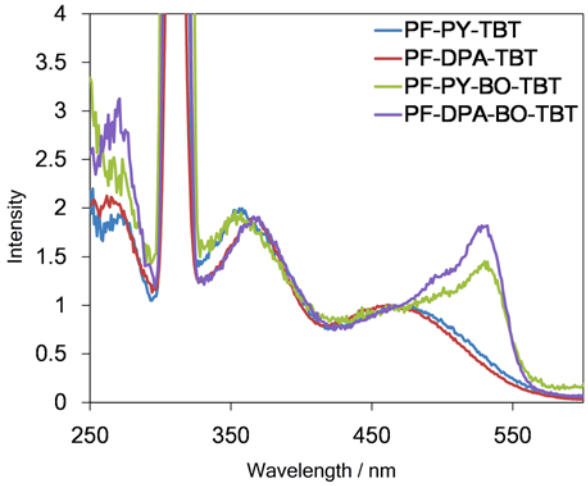

Figure S5. Normalized excitation spectra of the polymers in film states. Detection wavelength was at 625 nm.

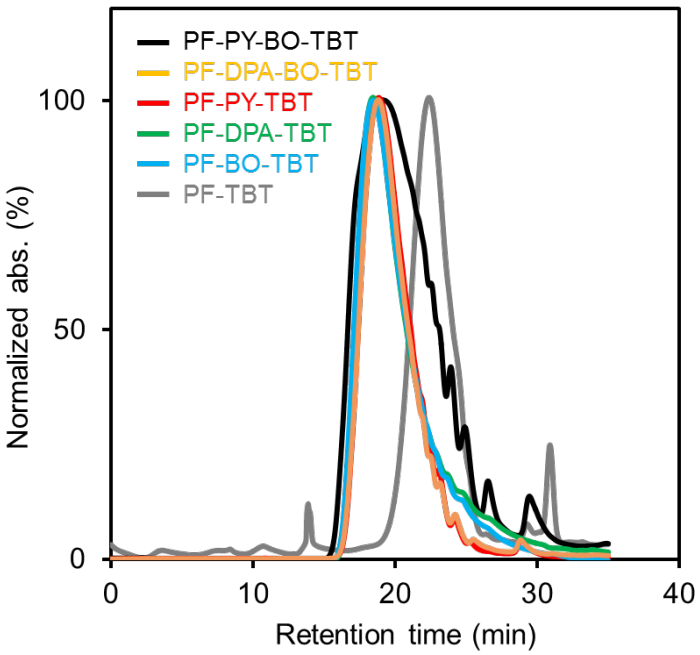

Figure S6. GPC profiles of the products in chloroform.